scientific reports

Check for updates

OPEN

Molecular modeling of CO_2 affecting competitive adsorption within anthracite coal

Lin Hong[1,2], Jiaxing Lin[1,2]✉, Dameng Gao[1,2,3] & Dan Zheng[1,2]

This study aimed to investigate the adsorption properties of CO_2, CH_4, and N_2 on anthracite. A molecular structural model of anthracite ($C_{208}H_{162}O_{12}N_4$) was established. Simulations were performed for the adsorption properties of single-component and multi-component gases at various temperatures, pressures, and gas ratios. The grand canonical ensemble Monte Carlo approach based on molecular mechanics and dynamics theories was used to perform the simulations. The results showed that the isotherms for the adsorption of single-component CO_2, CH_4, and N_2 followed the Langmuir formula, and the CO_2 adsorption isotherm growth gradient was negatively correlated with pressure but positively correlated with temperature. When the CO_2 injection in the gas mixture was increased from 1 to 3% for the multi-component gas adsorption, the proportion of CO_2 adsorption rose from 1/3 to 2/3, indicating that CO_2 has a competing-adsorption advantage. The CO_2 adsorption decreased faster with increasing temperature, indicating that the sensitivity of CO_2 to temperature is stronger than that of CH_4 and N_2. The adsorbent potential energies of CO_2, CH_4, and N_2 diminished with rising temperature in the following order: $CO_2 < CH_4 < N_2$.

Keywords Coal, Competitive adsorption, Energy distribution, Grand canonical ensemble Monte Carlo, Molecular dynamics

Technologies for infusing CO_2 or CO_2–N_2 mixtures into coal seams to replace CH_4 have gradually matured in recent years, improving CH_4 extraction rates and enabling the sequestration of large amounts of CO_2[1–4]. These technologies primarily utilize the different adsorption abilities of CO_2, CH_4, and N_2 on coal to improve the CH_4 extraction rate.

Gases in coal are mainly adsorbed physically. N_2 and CO_2 have a wide range of sources, where N_2 accounts for approximately 78% of the atmosphere while CO_2 is mainly generated through coal oxidation and combustion[5]. Scholars around the world have conducted multiple gas adsorption experiments[6–8] and Monte Carlo simulation studies[9–11] to investigate the adsorption characteristics of different gases on coal. The impact of temperature on gas adsorption has been investigated using the high-pressure volumetric method, which showed that low temperatures hinder gas adsorption on coal[12,13]. Li et al.[14] proposed the theory of the competitive adsorption of multiple gases using the low-temperature nitrogen adsorption method. Zhu et al.[15] experimentally verified that the maximum adsorption capacities of CO_2, CH_4, and N_2 on anthracite exceed those on bituminous coal at different temperatures. Xiao et al.[16,17] established the relationship between the coal adsorption capacity and temperature for CO_2, CH_4, and N_2. Cheng et al.[18,19] applied the grand canonical ensemble Monte Carlo method to investigate the adsorption properties of CO_2/N_2 on coal. Similarly, Wu et al.[20,21] investigated the microscopic mechanism of the competitive adsorption of coal-fired flue gas on coal. The research revealed the competitive adsorption behavior during the gas adsorption. Qu et al.[22] developed a macromolecular model of coal and used the grand canonical Monte Carlo (GCMC) and molecular dynamics (MD) molecular simulations to reveal the microscopic mechanisms of CO_2, O_2, and CH_4 adsorption and diffusion on coal molecules at different temperatures, pressures, and molar fractions. Gao et al.[23] analyzed the adsorption capacity of $CO_2/CH_4/N_2/H_2O$ on different molecular models of brown coal using molecular simulation. Wang et al.[24] used molecular simulation to examine the adsorption behavior of CH_4/CO_2 on oxidized coal deposits. Yu et al.[25] conducted experiments and simulations to examine the competitive adsorption mechanism of CO_2 and CH_4 on low-rank coal mirror groups. Bai et al.[26] performed a molecular simulation to investigate the kinetic mechanism of CO_2 and N_2

[1]College of Safety Science & Engineering, Liaoning Technical University, No. 188 Longwan South Street, Huludao 125105, Liaoning, China. [2]Key Laboratory of Mine Thermodynamic Disaster & Control of Ministry of Education, Liaoning Technical University, Huludao 125105, Liaoning, China. [3]Institute of Mine Safety Technology, China Academy of Safety Science and Technology, Beijing 100012, China. ✉email: m13596843024@163.com

replacement of CH_4. The results showed that CO_2 and N_2 mainly replaced CH_4 gas by occupying the adsorption site. Liu et al.[27] performed CO_2-ECBM tests on rectangular coal specimens and monitored the change patterns of pore pressure, gas flow, and outlet concentration with the amount of CO_2 injected; they found that infusing CO_2 into the coal body can effectively increase the CH_4 recovery. Li et al.[28] proposed a dynamic evolution model of coal permeability, which responded to the ECBM mining process and confirmed the technical feasibility of N_2-BCEM injection.

Other international scholars have also studied the adsorption properties of gases consisting of single components and multiple components. Using computer molecular simulations, Laurent et al.[29] investigated the absorbent behaviors of CO_2 and CH_4 in micropores. Perera et al.[30] investigated the adsorption capacity of two gases at three temperatures. Abunowara et al.[31] analyzed the characteristics of four coal sample adsorption gases in Malaysia using BET, XRD, FESEM, and other techniques, and the coal specimens exhibited a greater adsorption affinity for CO_2 than for CH_4 and N_2. Busch et al.[32] studied the gas adsorption of binary mixtures at a specific pressure using Langmuir's method, which provides an essential idea for this current study on the adsorption of ternary gas mixtures.

The studies highlighted above mainly focused on the adsorption characteristics of binary gas systems, confirming the advantage of CO_2 adsorption but ignoring the adsorption characteristics of ternary gas systems. In this article, we quantitatively analyzed the adsorption behavior of CO_2, CH_4, and N_2 on coal and the main influencing factors. The injection of different ratios of CO_2, CH_4, and N_2 into coal seams was simulated for the study.

Methodology

Molecular modeling of anthracite

The anthracite molecule ($C_{208}H_{162}O_{12}N_4$)[33] (illustrated in Fig. 1) was selected to study the adsorption properties of anthracite for CO_2, CH_4, and N_2. Geometry optimization, energy optimization, and simulated annealing were performed on the structure using the Forcite module in Materials Studio, and the optimized energy parameters are shown in Table 1 to obtain the lowest energy conformation, as shown in Fig. 2. The Amorphous cell module was used to put the two optimized anthracite molecular models into the computational cell (a = 18.607 Å, b = 18.607 Å, c = 18.607 Å), as shown in Fig. 3.

Simulation parameter setting

To simulate the adsorption of CO_2, CH_4, and N_2 on anthracite coal, we used a giant regular ensemble Monte Carlo simulation, selecting the Dreiding force field customized for computational accuracy, Charges selects QEq, the Ewald summation method for electrostatic interactions, and the atom-based method for van der Waals interactions. The temperatures used for the Fixed Pressure Task were 263.15 K, 273.15 K, 283.15 K, 293.15 K, 303.15 K, and 313.15 K, and the pressure ranged from 0.01 to 2 MPa.

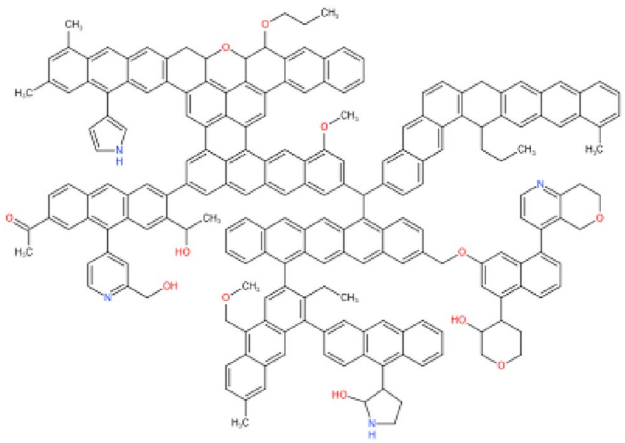

Figure 1. Molecular structure of anthracite.

	E_V (kcal/mol)				E_N (kcal/mol)		
E_{total} (kcal/mol)	E_B	E_A	E_T	E_I	E_{VAN}	E_E	E_H
343.389	107.235	86.263	126.985	3.024	525.086	− 5.337	− 0.0001

Table 1. Energy parameters of optimized coal molecular structure. E_V valence energy, E_B bond energy, E_A angle energy, E_T torsion energy, E_I inversion energy, E_N nonbond energy, E_{VAN} van der Waals energy, E_E electrostatic energy; E_H hydrogen bond energy.

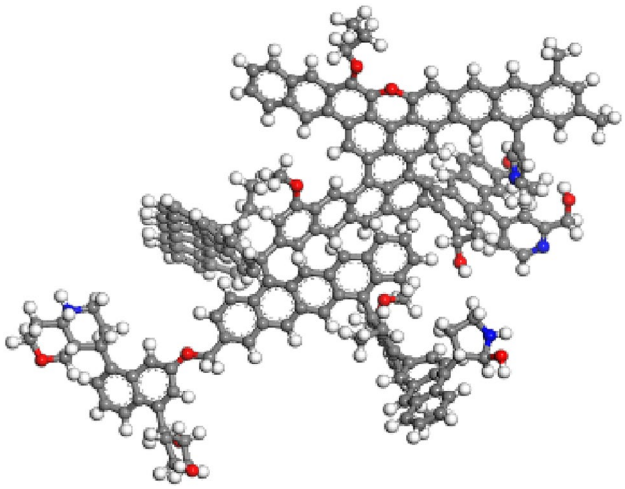

Figure 2. Molecular structural model of anthracite.

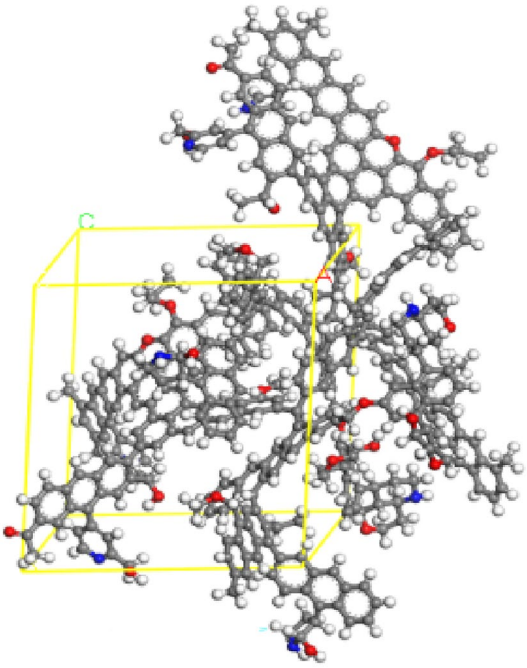

Figure 3. Pore structure model of anthracite.

Results and discussion

Single-component gas adsorption system

Figure 4 illustrates the adsorption isotherms of N_2, CO_2, and CH_4, as single-component gases under varying pressures and temperatures. As observed from the figure, at temperatures of 263.15 K, 273.15 K, 283.15 K, 293.15 K, 303.15 K, and 313.15 K and at pressures ranging from 0.01 to 2 MPa, the adsorption sites on the surface of the anthracite coal become more active with increasing temperature. Consequently, CO_2, CH_4, and N_2 are more readily detached from the coal surface, reducing the adsorption capacity. Similarly, Fig. 5 illustrates the variation of the CO_2, CH_4, and N_2 adsorption with temperature at a pressure of 0.1 MPa. At 263.15 K, a considerably larger number of adsorbed CO_2 molecules are in the anthracite molecular model than the number of CH_4 and N_2 molecules. With the increase of pressure from 0.01 MPa to 2 MPa in the system, the adsorption amount of CO_2, CH_4 and N_2 showed an upward trend, indicating that the elevated pressure can promote the adsorption of CO_2, CH_4 and N_2 by anthracite. The magnitude of adsorption at the same pressure is in the following order: $CO_2 > CH_4 > N_2$. This result can be explained as follows: first, the molecules of the three gases have different equivalent diameters, where the molecular diameter of CO_2 is 0.33 nm, that of N_2 is 0.368 nm, and that of CH_4 is 0.382 nm. Because the diameter of CO_2 molecule is small, the critical temperature and critical pressure of CO_2

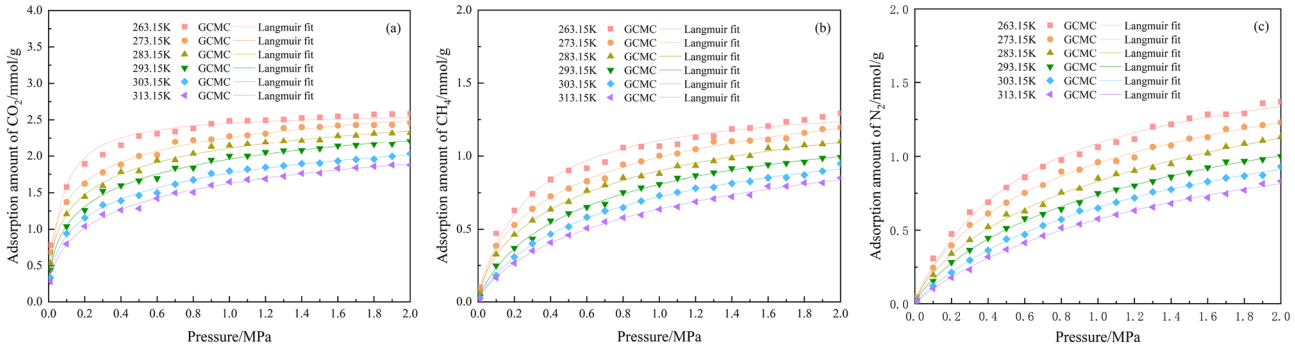

Figure 4. Isothermal adsorption curves for single-component: (**a**) CO_2, (**b**) CH_4 and (**c**) N_2.

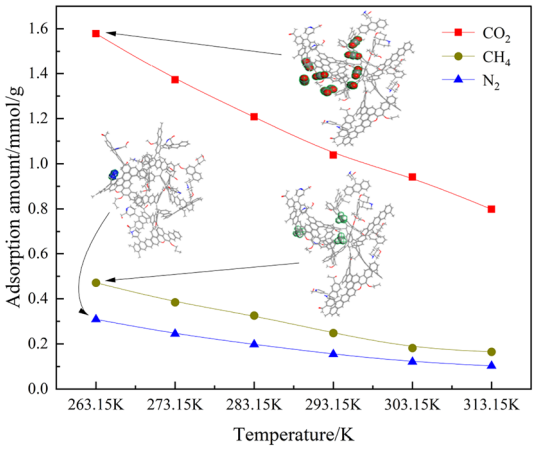

Figure 5. Variation of single-component gas adsorption with temperature at 0.1 MPa.

are larger, which makes the competitive adsorption advantage of CO_2 stronger than that of CH_4 and N_2 in the ternary gas system of CO_2, CH_4, and N_2, and therefore the anthracite molecules preferentially adsorb CO_2, so it leads to the adsorption amount of CO_2 is larger than that of CH_4 and N_2. Owing to the small difference between the molecular diameters of CH_4 and N_2, both have different polarization volume, where that of CH_4 is 4.48×10^{-30} m^3 and that of N_2 is 1.53×10^{-30} m^3. The molecules with a higher polarization volume are adsorbed more easily; thus, the amount of CH_4 adsorbed is larger than that of N_2. Secondly, the critical temperatures are different, the critical temperatures of CO_2, CH_4 and N_2 are 304 K, 191 K and 126 K. The size of the critical temperatures is $CO_2 > CH_4 > N_2$. As the critical temperature increases, the gas adsorption on the surface of the coal becomes faster and adsorbs more easily. Third, van der Waals forces also play a role: an increase in the pressure of the system is accompanied by an increase in the van der Waals energy, and the stronger the effect of the van der Waals force, the faster the adsorption. Take a temperature of 263.15 K as an example, the van der Waals energy data released by anthracite adsorption of CO_2, CH_4, and N_2 are shown in Table 2.

The isothermal adsorption curves of CO_2, CH_4, and N_2 at different pressure ranges have the form of Langmuir curves. Hence, the Langmuir formula was used to fit the isothermal adsorption curves of CO_2, CH_4, and N_2 for anthracite. The fitting results are presented in Table 3.

Gas	P/(MPa)	E_{VAN}/(kcal/mol)
CO_2	0.01	−49.447
	2	−87.397
CH_4	0.01	−6.198
	2	−37.306
N_2	0.01	0
	2	−28.859

Table 2. Van der Waals energy released by adsorption of CO_2, CH_4 and N_2 from anthracite coal at pressures of 0.01 MPa and 2 MPa.

Gas	T/K	Anthracite/(0.1–2 MPa)			Anthracite/(0.01–0.1 MPa)		
		k_1/(mmol/g)	k_2/(MPa^{-1})	R^2	k_1/(mmol/g)	k_2/(MPa^{-1})	R^2
CO_2	263.15 K	15.45930	12.41058	0.97808	10.22002	66.22327	0.94513
	273.15 K	14.83972	8.65084	0.95236	8.68364	60.82048	0.96314
	283.15 K	14.14749	7.24969	0.96037	8.12678	49.34100	0.95666
	293.15 K	13.49824	6.00503	0.96425	7.01259	47.49367	0.97249
	303.15 K	12.34502	5.50192	0.94853	6.84291	32.66120	0.98443
	313.15 K	11.75505	4.62049	0.95514	5.98387	29.65065	0.98381
CH_4	263.15 K	8.13773	3.74307	0.97177	5.32766	13.39820	0.98118
	273.15 K	7.92619	2.85655	0.98222	3.73444	10.85104	0.98689
	283.15 K	7.44071	2.51863	0.98498	4.35184	7.07093	0.98279
	293.15 K	7.19663	1.94083	0.99350	4.06383	5.81027	0.98742
	303.15 K	6.84858	1.62792	0.99534	2.98200	5.26464	0.98378
	313.15 K	6.49959	1.39296	0.99171	4.67810	2.40749	0.99387
N_2	263.15 K	10.05641	1.69437	0.99118	4.58182	6.39676	0.99840
	273.15 K	9.33844	1.51337	0.99350	5.15792	3.97161	0.99735
	283.15 K	9.09189	1.18631	0.99201	4.62266	3.30171	0.99848
	293.15 K	8.46873	1.06177	0.99591	5.24324	2.09114	0.99755
	303.15 K	8.43825	0.83123	0.99830	4.58101	1.84693	0.99772
	313.15 K	8.01405	0.71803	0.99745	18.97877	0.32407	0.99886

Table 3. Fitting parameters of the Langmuir model.

The fitting results show that the linear correlation coefficient R^2 was greater than 0.94 in all cases, indicating good fitting and confirming the reliability of the simulated data. The adsorption constants k_1, k_2 decrease with increasing temperature; the adsorption amount also decreases, indicating that low temperatures are favorable for CH_4 adsorption.

Figure 4 shows that the adsorption isotherm growth gradient of CO_2, CH_4, and N_2 within the pressure range of 0.01–0.1 MPa is considerably larger than that within the pressure ranges of 0.1–1 MPa and 1–2 MPa. Therefore, CO_2 was used as an example to calculate the adsorption isotherm growth gradients of the gases at different temperatures, as shown in Table 4.

At different temperatures, the growth gradients of CO_2 adsorption isotherms were 1.985–2.809 for pressures of 0.01–0.1 MPa, 1.468–1.892 for pressures of 0.1–1.0 MPa, and 0.975–1.035 for pressures of 1.1–2.0 MPa. These results show that the CO_2 adsorption isotherm growth gradient is the largest and the adsorption rate is the fastest in the pressure range of 0.01–0.1 MPa. This phenomenon occurs because of the large number of adsorption sites on the anthracite surface. Initially, CO_2, CH_4, and N_2 are easily adsorbed on these sites, resulting in a faster adsorption rate, but the gas concentration increases while the adsorption sites are gradually saturated, causing the adsorption rate to decelerate until it reaches equilibrium. Therefore, the larger the growth gradient of the adsorption isotherm, the faster the adsorption rate. This behavior occurs because the growth gradient represents the rate of gas adsorption; the faster the adsorption rate, the greater the number of adsorption sites on the anthracite surface.

Multi-component gas adsorption system

Adsorption amount

The single-component gas adsorption shows that CO_2 has certain adsorption advantages over CH_4 and N_2. Different proportions of CO_2, CH_4, and N_2 were added to the anthracite pore model. As the adsorption rate of the gases with pressure ranging from 0.01 to 0.1 MPa is the fastest in the single-component gas adsorption system, the adsorption characteristics of the three gases are discussed for a pressure of 0.1 MPa. The simulation results are shown in Fig. 6.

A comparison of Fig. 6a–c shows that adding the same ratio of CH_4 and different ratios of CO_2 and N_2 to the anthracite molecule with the temperature of 263.15 K, the relative CO_2 adsorption increases from 0.20 to

P/MPa	T/K					
	263.15	273.15	283.15	293.15	303.15	313.15
0.01–0.1	1.985	2.017	2.262	2.307	2.768	2.809
0.1–1.0	1.468	1.553	1.644	1.757	1.790	1.892
1.1–2.0	0.975	1.000	1.009	1.027	1.029	1.035

Table 4. Growth gradient of CO_2 adsorption isotherms at different temperatures.

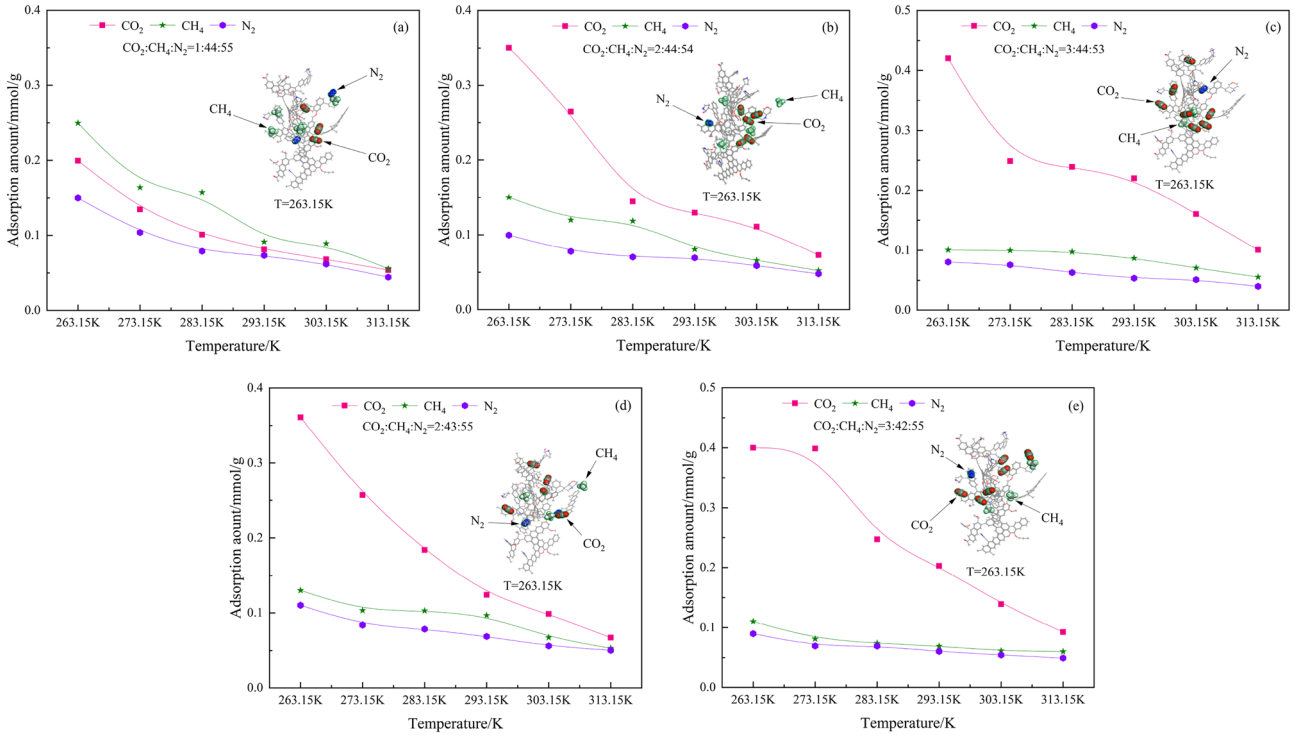

Figure 6. Variation of multi-component gas adsorption amount with temperature at 0.1 MPa.

0.42 mmol/g as the CO_2 injection increases from 1 to 3%; The relative adsorption of the same proportion of CH_4 decreases with the gradual increase in the CO_2 injection. The relative adsorption of CH_4 decreases from 0.25 to 0.10 mmol/g while that of N_2 in different proportions decreases from 0.15 to 0.08 mmol/g. A comparison of the plots in Fig. 6a,d and e shows that at the temperature of 263.15 K, injecting the same proportion of N_2 and different proportions of CO_2 and CH_4 increases the relative adsorption of CO_2 with increasing amount of injected gas from 0.20 to 0.40 mmol/g. The relative adsorption of CH_4 decreases from 0.25 to 0.11 mmol/g with decreasing CH_4 injection, and the relative adsorption of equal proportions of N_2 decreases from 0.15 to 0.09 mmol/g. These results show that the adsorption sensitivity of CO_2 is very strong, and the relative CO_2 adsorption increases rapidly when the CO_2 injection increases from 1 to 3%, which far exceeds the relative adsorption of CH_4 and N_2. Second, the relative adsorption of CH_4 decreases slowly as CO_2 injection increases in the system, which is because CO_2 has certain adsorption advantages and a stronger adsorption capacity than CH_4. Hence, CO_2 is preferentially adsorbed, decreasing the relative adsorption of CH_4. Third, different proportions of N_2 and equal proportions of N_2 have less effect on changes in the adsorption amount of the system, indicating that N_2 adsorption is more stable. The amount of gas adsorbed is affected not only by temperature and gas injections, but also by the adsorption potential. When a gas is adsorbed on the surface of the coal body, the adsorbent is also attracted to the adsorbate; the closer to the surface, the greater the gravitational force, which is the adsorption potential; thus, the adsorption amount is also related to the adsorption potential.

Adsorption potential

Polanyi[34] and Dubinin[35] proposed the adsorption potential theory. The theory posits that an adsorption potential field encircles a solid, and gas molecules are adsorbed within this field through the influence of attractive forces. Consequently, the connection between the adsorption potential and adsorption amount was used to analyze the adsorption features of three gases: CO_2, CH_4, and N_2.

According to Polanyi, the relationship between adsorption potential and pressure is as follows:

$$\varepsilon = RT\ln\frac{P_0}{P}. \tag{1}$$

In this context, ε represents the adsorption potential [J/mol]; R represents the ideal gas constant, taken as 8.3144 J/(mmol·K); T represents the absolute temperature [K]; P0 represents the vapor pressure at saturation of the gas corresponding to temperature T [MPa]; and P represents the pressure [MPa].

According to Dubinin, the formula for calculating P0 is,

$$P_0 = P_c\left(\frac{T}{T_C}\right)^2. \tag{2}$$

In this context, Pc represents the critical pressure; the critical pressures of CO_2, CH_4, and N_2 are taken as 7.38 MPa, 4.60 MPa, and 3.40 MPa, respectively. Tc represents the critical temperature, and the critical temperatures of CO_2, CH_4, and N_2 are taken as 304.13 K, 190.56 K, and 126.20 K, respectively.

When we combine the simulation data and substitute Eq. (2) into Eq. (1), the relationship between the adsorption amount and adsorption potential energy of multi-component gases at different temperatures can be calculated, which is illustrated in Fig. 7.

Figure 7a and b demonstrate that by injecting the same proportion of CH_4 and N_2 into the system, the CO_2 adsorption increases rapidly at the temperature of 263.15 K. This phenomenon occurred because of the increased CO_2 concentration in the system resulting from the increase in CO_2 injection in the system from 1 to 3%. Because of the adsorption advantage of CO_2 itself over CH_4 and N_2, the relative adsorption of CO_2 rises rapidly. When the system temperature increases from 263.15 to 283.15 K, the CO_2 adsorption rapidly decreases because CO_2 is more temperature-sensitive than CH_4 and N_2. The adsorption levels off when the temperature increases from 283.15 to 313.15 K. This is because the adsorption decreases with increasing temperature, which is consistent with the conclusion of the single-component gas adsorption. The adsorption potential energy of CO_2 increases from 8.78 to 11.35 kJ/mol, that of CH_4 from 9.79 to 12.56 kJ/mol, and that of N_2 from 10.93 to 13.91 kJ/mol, indicating that the adsorption potential energy of each gas component increases with increasing temperature, and the adsorption potential energy of the gas components follows the order: $CO_2 < CH_4 < N_2$. As shown in Fig. 7a, CO_2 adsorption decreases from 1.01 to 0.24 mmol/g, CH_4 adsorption decreases from 0.48 to 0.16 mmol/g, and N_2 adsorption drops from 0.31 to 0.13 mmol/g. As shown in Fig. 7b, CO_2 adsorption decreases from 0.85 to 0.22 mmol/g, CH_4 adsorption decreases from 0.47 to 0.13 mmol/g, N_2 adsorption decreases from 0.31 to 0.13 mmol/g, and the adsorption amounts of the gas components are in the order of $CO_2 > CH_4 > N_2$. Therefore, the adsorption amount has a negative correlation with the adsorption potential energy, i.e. the quantity of gas adsorbed reduces as the adsorption potential energy increases. From a thermodynamic perspective, anthracite adsorbs the most CO_2, followed by CH_4 and N_2. This phenomenon occurs because a rise in temperature increases the thermal movement of the solid surface molecules, weakening the intermolecular interaction forces and, consequently, reducing the surface energy. Thus, the CO_2, CH_4, and N_2 molecules are not easily adsorbed on the surface of the coal molecules, which reduces the adsorption amount.

Potential energy distribution

The potential energy distribution of the anthracite adsorption of CO_2, CH_4, and N_2 was obtained through a simulation, and the relationship between the preferential adsorption potential and the amount of gas injected was analyzed. The results are illustrated in Fig. 8 for the pressure of 0.1 MPa and temperature of 263.15 K. The data on the initial potential energy distribution of the gases are shown in Table 5.

Adsorption energy is the energy produced during adsorption. Molecules decelerate and eventually stop at the surface of the adsorption medium during adsorption, which releases some energy. Thus, the greater the absolute value of the adsorption energy, the greater the intermolecular interactions and preferential adsorption.

A comparison of (a) and (b) in Fig. 8 shows that for different injection ratios of CO_2, CH_4, and N_2 into the system, the absolute magnitude of the potential energy peak of CO_2 increases with the increasing quantity of gas injected the system. In the two gas systems with certain CH_4 and N_2 ratios, the potential energy peak of the optimal adsorption site of CO_2 decreases from − 8.85 kcal/mol to − 9.65 and − 9.15 kcal/mol, respectively. The potential energy peak of the optimal adsorption site of CH_4 decreased from − 3.95 kcal/mol to − 5.05 and − 6.95 kcal/mol, respectively. The potential energy peak of the optimal adsorption site of N_2 decreased from − 3.65 kcal/mol to − 4.65 and − 3.95 kcal/mol, respectively. A comparison of (a) and (b) shows that the optimal adsorption site for injecting the same proportion of CH_4 into the system is higher than that of N_2; thus, the preferential adsorption potential of CO_2 is greater than that of CH_4, and that of CH_4 is greater than that of N_2. This result is consistent with the order of magnitude of the amount of the three gases adsorbed. The absolute values

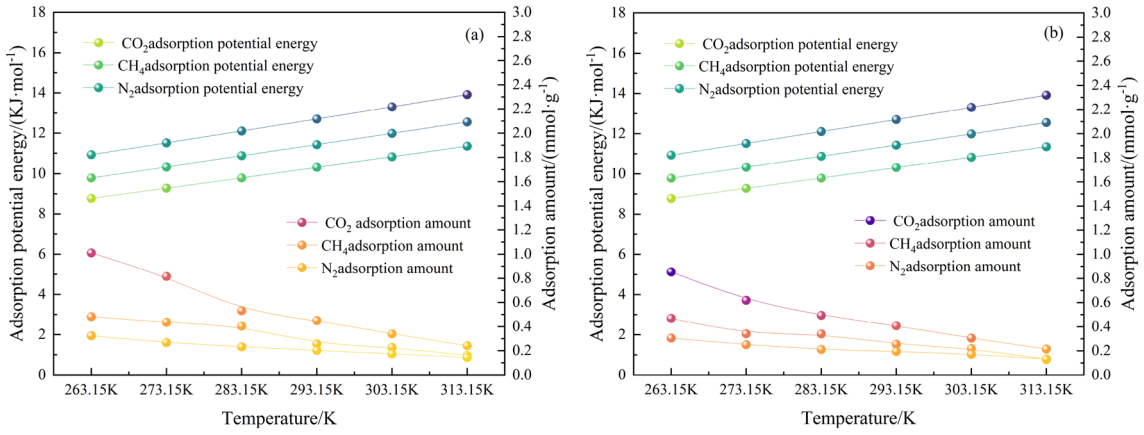

Figure 7. Curves of relationship between adsorption amount and adsorption potential energy of multi-component gases at different temperatures. (**a**) is injected in the ternary gas system with the same proportion of CH_4, (**b**) is injected in the ternary gas system with the same proportion of N_2.

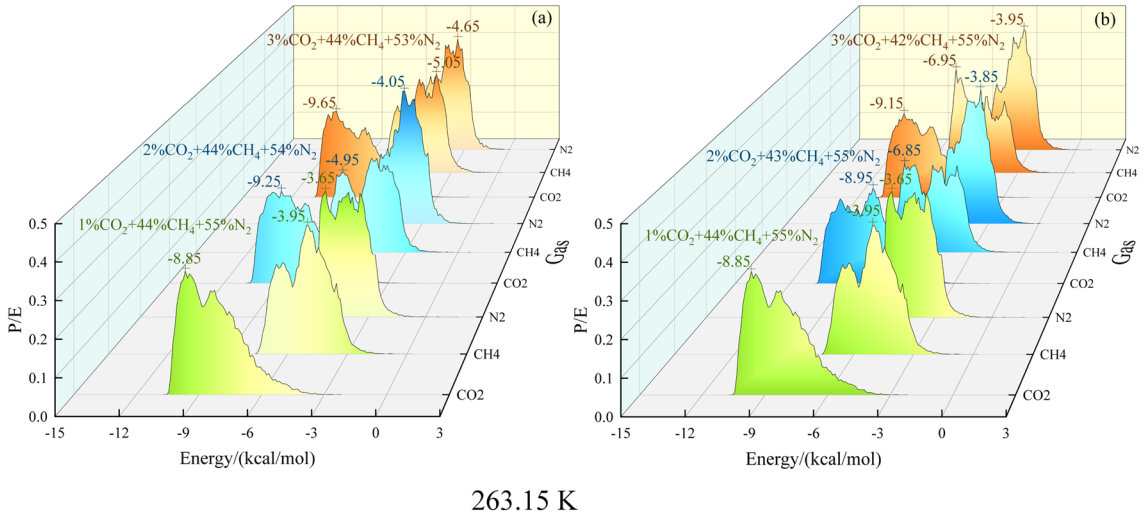

263.15 K

Figure 8. Potential energy distribution of multi-component gas. (**a**) and (**b**) are the potential energy distributions analyzed in the system of CH_4 and N_2 in the same proportions, with the initial ratio of CO_2, CH_4, and N_2 all being 1:44:55.

No	Initial adsorbate potential for injection of equal proportions of CH_4/(kcal/mol)			No	Initial adsorbate potential for injection of equal proportions of N_2/(kcal/mol)		
	CO_2	CH_4	N_2		CO_2	CH_4	N_2
1	− 10.65	− 7.45	− 6.05	1	− 10.75	− 7.65	− 6.05
2	− 10.85	− 7.75	− 6.15	2	− 10.95	− 7.75	− 6.15
3	− 10.95	− 7.85	− 6.35	3	− 11.05	− 7.95	− 6.25

Table 5. Potential energy distribution of initial adsorbates injected with equal proportions of CH_4 (a) and equal proportions of N_2 (b) in a ternary gas system.

of the potential energy peaks for both CH_4 and N_2 showed a rising pattern with the increase in CO_2 injection; hence, CO_2 can promote the adsorption behavior of CH_4 and N_2 on anthracite.

Conclusions

(1) The adsorption behavior of the single-component gas system is in accordance with Langmuir's law of adsorption, and the values of adsorption constants k_1, k_2 are generally negatively correlated with temperature. From the perspective of the adsorption rate, CO_2, CH_4, and N_2 attained the fastest adsorption rate in the single-component gas adsorption system at temperatures of 263.15 K, 273.15 K, 283.15 K, 293.15 K, 303.15 K, and 313.15 K, as well as pressures in the range of 0.01 to 2 MPa. In different pressure ranges, the adsorption rate of CO_2 increased with increasing temperature because adsorption is typically exothermic, and when the adsorption process has not reached equilibrium, elevated temperatures accelerate the rate of adsorption. The adsorption amount was positively correlated with pressure and negatively correlated with temperature, and the adsorption amounts were in this order of magnitude: $CO_2 > CH_4 > N_2$.

(2) In the multi-component gas system, at the same pressure, the proportion of the relative adsorption amount of CO_2 in the system increased from 1/3 to 2/3 with the increase in CO_2 injection from 1 to 3%, whereas the relative adsorption of CH_4 and N_2 decreased. The relative CO_2 adsorption was positively correlated with the amount of gas injected but negatively correlated with temperature. The relative adsorption amounts were in this order of magnitude: $CO_2 > CH_4 > N_2$.

(3) In the multi-component gas system, under identical pressures, the adsorption potential energy of CO_2, CH_4, and N_2 at 263.15 K was 8.78 kJ/mol, 9.79 kJ/mol, and 10.93 kJ/mol, respectively, with the values increasing with increasing temperature. The adsorption potential energy of CO_2, CH_4, and N_2 was positively correlated with temperature and negatively correlated with the adsorption amount. The adsorption potential energy of the three gases was in this order of magnitude: $CO_2 < CH_4 < N_2$.

(4) In the multi-component gas system, at the same temperature and pressure, the potential energy peaks of CO_2, CH_4, and N_2 were − 8.85 kcal/mol, − 3.95 kcal/mol, and − 3.65 kcal/mol, respectively, and the absolute values at the optimal adsorption sites were in this order of magnitude: $CO_2 > CH_4 > N_2$. The absolute values of the potential energy peaks of the optimal adsorption sites for CH_4 and N_2 increased as the injection of

CO_2 into the system increased. Furthermore, the preferential adsorption potentials followed the order of $CO_2 > CH_4 > N_2$.

Data availability

All data supporting the findings of this study are available from the corresponding author Jiaxing Lin upon request.

Received: 14 January 2024; Accepted: 29 March 2024
Published online: 30 March 2024

References

1. Fan, N. *et al.* Numerical study on enhancing coalbed methane recovery by injecting N_2/CO_2 mixtures and its geological significance. *Energy Sci. Eng.* **8**, 1104–1119 (2020).
2. Jeong, S. R. *et al.* Review of the adsorption equilibria of CO_2, CH_4, and their mixture on coals and shales at high pressures for enhanced CH_4 recovery and CO_2 sequestration. *Fluid Phase Equil.* **564**, 113591 (2023).
3. Lin, J., Ren, T., Cheng, Y. P., Nemcik, J. & Wang, G. D. Cyclic N_2 injection for enhanced coal seam gas recovery: A laboratory study. *Energy* **188**, 116115 (2019).
4. Talapatra, A., Halder, S. & Chowdhury, A. I. Enhancing coal bed methane recovery: Using injection of nitrogen and carbon dioxide mixture. *Petrol. Sci. Technol.* **39**, 49–62 (2021).
5. Deng, J., Xiao, Y., Li, Q. W., Lu, J. H. & Wen, H. Experimental studies of spontaneous combustion and anaerobic cooling of coal. *Fuel* **157**, 261–269 (2015).
6. Davarpanah, A. & Mirshekari, B. Experimental investigation and mathematical modeling of gas diffusivity by carbon dioxide and methane kinetic adsorption. *J. Ind. Eng. Chem. Res.* **58**, 12392–12400 (2019).
7. Xue, Y. *et al.* Experimental investigation of mechanical properties, impact tendency, and brittleness characteristics of coal mass under different gas adsorption pressures. *Geomech. Geophys. Geo-Energy Geo-Resour.* https://doi.org/10.1007/s40948-022-00439-6 (2022).
8. Zhu, H. Q., Guo, S., Xie, Y. Y. & Zhao, H. R. Molecular simulation and experimental studies on CO_2 and N_2 adsorption to bituminous coal. *Environ. Sci. Pollut. Res.* **28**, 15673–15686 (2021).
9. Hao, M., Qiao, Z., Zhang, H., Wang, Y. L. & Li, Y. L. Thermodynamic analysis of $CH_4/CO_2/N_2$ adsorption on anthracite coal: Investigated by molecular simulation. *Energy Fuels* **35**, 4246–4257 (2021).
10. Hao, M., Zhao, Y. C., Wei, C. M., Zhang, H. & Wang, Y. L. Multi-component gases competitive adsorption on residual coal under goaf conditions based on Monte Carlo simulation. *Chem. Phys. Lett.* **771**, 138557 (2021).
11. Wu, S. Y., Deng, C. B. & Wang, X. F. Molecular simulation of flue gas and CH_4 competitive adsorption in dry and wet coal. *J. Nat. Gas Sci. Eng.* **71**, 102980 (2019).
12. Qu, G. *et al.* Experiment and molecular simulation study on the adsorption of CH_4 and CO_2 by coal with high-metamorphic. *J. Saf. Environ.* **22**, 142–147 (2022).
13. Zhang, Z., Zhao, D., Zhang, C., Chen, Y. & Tang, C. Isothermal adsorption/desorption characteristics of soft coal at different temperatures. *J. Liaoning Tech. Univ. (Nat. Sci.)* **40**, 510–517 (2021).
14. Li, S., Li, Z., Liu, P., Bai, Y. & Yan, M. Experimental study of competitive adsorption characteristics and mechanism of $N_2/CH_4/CO_2$ mixture on coal. *J. China Univ. Min. Technol.* **52**, 446–456 (2023).
15. Zhu, C. J. *et al.* Experimental comparison of CO_2, CH_4, and N_2 adsorption capacity on typical Chinese coals at different temperatures. *Energy Sour. A Recov. Util. Environ. Effects* https://doi.org/10.1080/15567036.2020.1806954 (2020).
16. Xiao, T. *et al.* Experimental research on adsorption characteristics of N_2, CH_4, and CO_2 in coal under different temperatures and gas pressures. *Energy Sci. Eng.* **11**, 637–653 (2023).
17. Zhou, W. *et al.* Experimental study of the effects of gas adsorption on the mechanical properties of coal. *Fuel* **281**, 118745 (2020).
18. Cheng, G., Tang, X. & Si, J. Adsorption analysis of CO_2/N_2 in bituminous coal and anthracite. *J. North China Inst. Sci. Technol.* **20**, 34–43 (2023).
19. Zhu, H. Q. *et al.* Molecular simulation study on adsorption and diffusion behaviors of CO_2/N_2 in lignite. *Acs Omega* **5**, 29416–29426 (2020).
20. Wu, S. Y., Jin, Z. X. & Deng, C. B. Molecular simulation of coal-fired plant flue gas competitive adsorption and diffusion on coal. *Fuel* **239**, 87–96 (2019).
21. Zhou, W. N. *et al.* Molecular simulation of $CO_2/CH_4/H_2O$ competitive adsorption and diffusion in brown coal. *RSC Adv.* **9**, 3004–3011 (2019).
22. Qu, L. A., Wang, Z. Z. & Liu, L. Molecular simulation study based on adsorption of gas (CO_2, O_2, CH_4) on Coal. *Fire-Switzerland* **6**, 355 (2023).
23. Gao, D. M., Hong, L., Wang, J. R. & Zheng, D. Molecular simulation of gas adsorption characteristics and diffusion in micropores of lignite. *Fuel* **269**, 117443 (2020).
24. Wang, S., Hu, Y., Yang, X. S., Liu, G. D. & He, Y. R. Examination of adsorption behaviors of carbon dioxide and methane in oxidized coal seams. *Fuel* **273**, 117599 (2020).
25. Yu, S., Bo, J. & Li, J. H. Retraction: Simulations and experimental investigations of the competitive adsorption of CH_4 and CO_2 on low-rank coal vitrinite (Retraction of Vol 23, art no 280, 2017). *J. Mol. Model.* https://doi.org/10.1007/s00894-019-4074-8 (2019).
26. Bai, Y., Lin, H. F., Li, S. G., Yan, M. & Long, H. Molecular simulation of N_2 and CO_2 injection into a coal model containing adsorbed methane at different temperatures. *Energy* **219**, 119686 (2021).
27. Liu, Z. D., Cheng, Y. P., Wang, Y. K., Wang, L. & Li, W. Experimental investigation of CO_2 injection into coal seam reservoir at in-situ stress conditions for enhanced coalbed methane recovery. *Fuel* **236**, 709–716 (2019).
28. Li, B., Zhang, J. X., Ding, Z. B., Wang, B. & Li, P. A dynamic evolution model of coal permeability during enhanced coalbed methane recovery by N_2 injection: Experimental observations and numerical simulation. *RSC Adv.* **11**, 17249–17258 (2021).
29. Laurent, B. *et al.* Adsorption-induced deformation of microporous materials: Coal swelling induced by CO_2-CH_4 competitive adsorption. *Langmuir ACS J. Surf. Colloids* **28**, 2659–2670 (2012).
30. Perera, M. S. A., Ranjith, P. G., Choi, S. K., Airey, D. & Weniger, P. Estimation of gas adsorption capacity in coal: A review and an analytical study. *Int. J. Coal Prep. Util.* **32**, 25–55 (2012).
31. Abunowara, M. *et al.* Experimental measurements of carbon dioxide, methane and nitrogen high-pressure adsorption properties onto Malaysian coals under various conditions. *Energy* https://doi.org/10.1016/j.energy.2020.118575 (2020).
32. Busch, A. & Gensterblum, Y. CBM and CO_2-ECBM related sorption processes in coal: A review. *Int. J. Coal Geol.* **87**, 49–71 (2011).
33. Li, B. Research of adsorption-deformation-seepage-diffusion characteristics of $CO_2/CH_4/N_2$ in coals with different coal ranks (in Chinese). Dissertation for Doctor Degree, Liaoning Technical University (2022). doi:https://doi.org/10.27210/d.cnki.glnju.2022.000869.

34. Polanyi, M. The potential theory of adsorption: Authority in science has its uses and its dangers. *Science* **141**, 1010–1013 (1963).
35. Dubinin, M. The potential theory of adsorption of gases and vapors for adsorbents with energetically nonuniform surfaces. *Chem. Rev.* **60**, 235–241 (1960).

Acknowledgements
The authors would like to thank all the reviewers who participated in the review, as well as MJEditor (www.mjeditor.com) for providing English editing services during the preparation of this manuscript.

Author contributions
The data were analyzed by H.L. and G. D., Z. D. analyzed the images, and L.J. wrote the manuscript.

Funding
This work is supported by the National Natural Science Foundation of China (Grant No.52074147), Liaoning Natural Science Foundation of China (Grant No. LJKQZ20222334).

Competing interests
The authors declare no competing interests.

Additional information
Correspondence and requests for materials should be addressed to J.L.

Reprints and permissions information is available at www.nature.com/reprints.

Publisher's note Springer Nature remains neutral with regard to jurisdictional claims in published maps and institutional affiliations.